

Regional climate change in the Middle East and impact on hydrology in the Upper Jordan catchment

**HARALD KUNSTMANN¹, PETER SUPPAN¹,
ANDREAS HECKL¹ & ALON RIMMER²**

¹ Institute for Meteorology and Climate Research (IMK-IFU), Forschungszentrum Karlsruhe, Kreuzeckbahnstraße 19, D-82467 Garmisch-Partenkirchen, Germany
harald.kunstmann@imk.fzk.de

² Kinneret Limnological Laboratory, Israel Oceanographic & Limnological Research Ltd, PO Box 447, Migdal 14950, Israel

Abstract The impact of climate change on water availability in the Middle East and the Upper Jordan catchment (UJC) is investigated by dynamic downscaling of ECHAM4 time slices and subsequent hydrological modelling. Two time slices (1961–1990 and 2070–2099) of the global climate scenario B2 of ECHAM4 were dynamically downscaled with the meteorological model MM5 in two nesting steps of 54 km and 18 km resolution. The meteorological fields were used to drive a physically-based hydrological model, computing in detail the surface and subsurface water flow and water balance of the UJC. The results of the joint regional climate-hydrology simulations indicate mean annual temperature increases of up to 4.5°C, and 25% decreases in mean annual precipitation in the mountainous part of the UJC. Total runoff at the outlet of the catchment is predicted to decrease by 23%, and is accompanied by a significant decrease of groundwater recharge.

Key words climate change; dynamic downscaling; Middle East; hydrological modelling; water availability

INTRODUCTION

Sufficient freshwater availability is a central prerequisite for agricultural and industrial development in the water scarce environment of the eastern Mediterranean and Middle East (EM/ME). Political peace in the region is strongly linked to the satisfactory compliance of increasing water demands. Sustainable management of water resources requires scientifically sound decisions on future freshwater availability, in particular under global climate change and increasing greenhouse gas emissions. Behind this background, the impact of climate change on water availability in EM/ME, and in particular the Jordan River catchment, is investigated within the framework of the GLOWA-Jordan River project (<http://www.glowa-jordan-river.de>). This article focuses on the Upper Jordan River catchment (UJC) which provides a third of freshwater resources in Israel.

REGIONAL CLIMATE MODELLING FOR THE EASTERN MEDITERRANEAN/MIDDLE EAST AND THE JORDAN RIVER REGION

The Jordan catchment is located within a narrow transition zone of only a couple of hundred kilometres, with a Mediterranean climate in the west and an arid climate

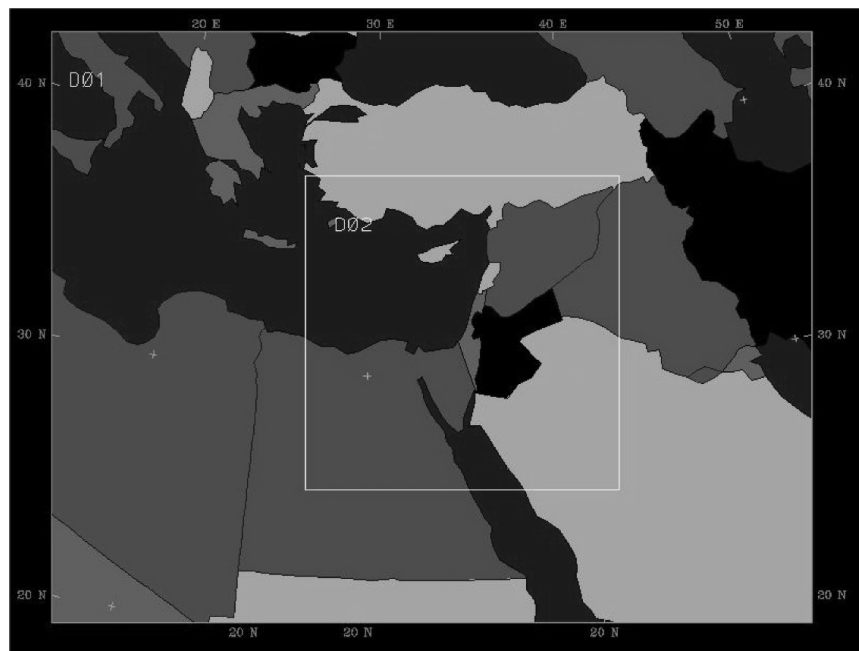


Fig. 1 ECHAM4 global climate scenarios were dynamically downscaled with MM5 using two nests of 54 km and 18 km resolution.

(Negev Desert) to the east/southeast. The non-hydrostatic model MM5 (Grell *et al.*, 1994) is applied to model atmospheric processes in the region. To investigate the impact of global warming on the water availability in the EM/ME and in particular the UJC, the global climate scenario B2 of ECHAM4 was dynamically downscaled from 2.8° (roughly 300 km) in two nesting steps of 54 km and 18 km resolution (Fig. 1). Emission scenario B2 describes a world with continuously increasing global population, intermediate levels of economic development and emphasis on local solutions to economic, social and environmental sustainability.

The MM5 model configuration is as follows: model top is set at 100 mbar. Terrain following coordinates and 26 vertical layers are used. Convective, subgrid-scale precipitation was parameterized according to Grell *et al.* (1994). Microphysics was calculated according to Reisner *et al.* (1998) which differentiates between water vapour, snow, ice, cloud water, rain water and graupel. The turbulent fluxes in the planetary boundary layer were parameterized according to Hong & Pan (1996). Feedback between soil moisture, temperature, vegetation, soil properties and atmosphere were accounted for by applying MM5 fully 2-way coupled with the Oregon State University-Land Surface Model (OSU-LSM) (Chen & Dudhia, 2001).

Two 30-year time slices (1961–1990 and 2070–2099) of the global climate model ECHAM4 were processed. Figure 2 shows a comparison between simulated and observed mean annual precipitation for 41 meteorological stations (located in domain 2 of Fig. 1) indicating that the simulations reproduce observed climate satisfactorily, albeit that slight under- and overestimations occur. In general it is concluded that the derived trends of expected climate change and the differences between the two time slices are estimated more reliably than the absolute numbers of each respective time slice.

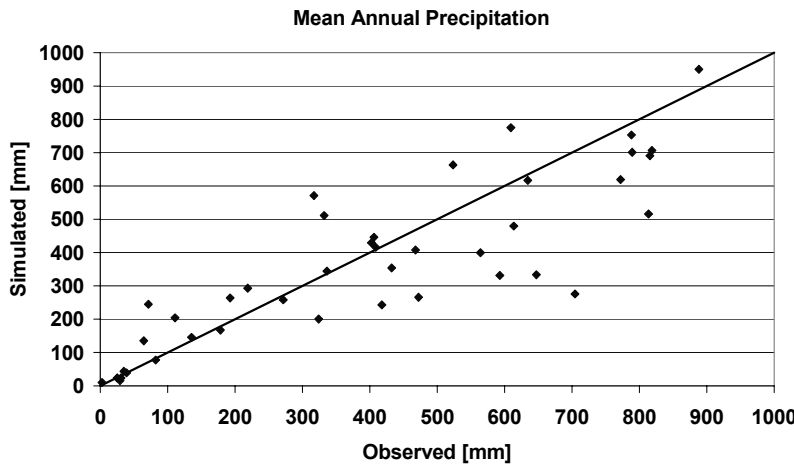


Fig. 2 Comparison of modelled (1961–1990) and long-term observed (1961–1990) mean annual precipitation (mm) for 41 meteorological stations in domain 2.

Figure 3 shows predicted changes in mean annual temperature and mean annual precipitation based on the results of the 18 km resolution (domain 2). It is seen that temperature increases of up to 4°C are expected and the mean annual precipitation is decreased by as much as 30% in specific regions.

The temporal distributions of precipitation change in four different subregions (A–D) are shown in Fig. 4. For all four subregions, a significant decrease in winter precipitation and a slight increase in precipitation during spring time are predicted.

In order to investigate the impact of anticipated climate change on the terrestrial water availability, the regional climate modelling results were used to drive a distributed, physically-based hydrological model of the UJC. The approach follows closely Kunstmann *et al.* (2004), who applied this methodology of 1-way coupled regional climate-hydrology simulations to Alpine catchments.

DISTRIBUTED HYDROLOGICAL MODELLING OF THE UPPER JORDAN CATCHMENT

The distributed hydrological model WaSiM (Schulla & Jasper, 2000) was applied in $90 \times 90 \text{ m}^2$ horizontal resolution to perform the hydrological simulations of the UJC. WaSiM uses physically-based algorithms for the majority of the process descriptions: an infiltration approach after Green & Ampt (1911), estimation of saturation time after Peschke (1987), and solving of the Richards equation (Richards, 1931; Phillip, 1969) for the description of the soil water fluxes in the unsaturated zone (Jasper *et al.*, 2002). The dependence of the suction head and the hydraulic conductivity on soil moisture content is parameterized according to van Genuchten (1976). Interflow is calculated in defined different soil layers, depending on suction, drainable water content, hydraulic conductivity, and gradient. Surface runoff is routed to the sub-basin outlet using a subdivision of the basin into flow time zones. For considering retention, a single linear storage approach is applied to the surface runoff in the last flow time zone. Translation and retention of interflow is treated accordingly. Actual evapotranspiration is soil- and

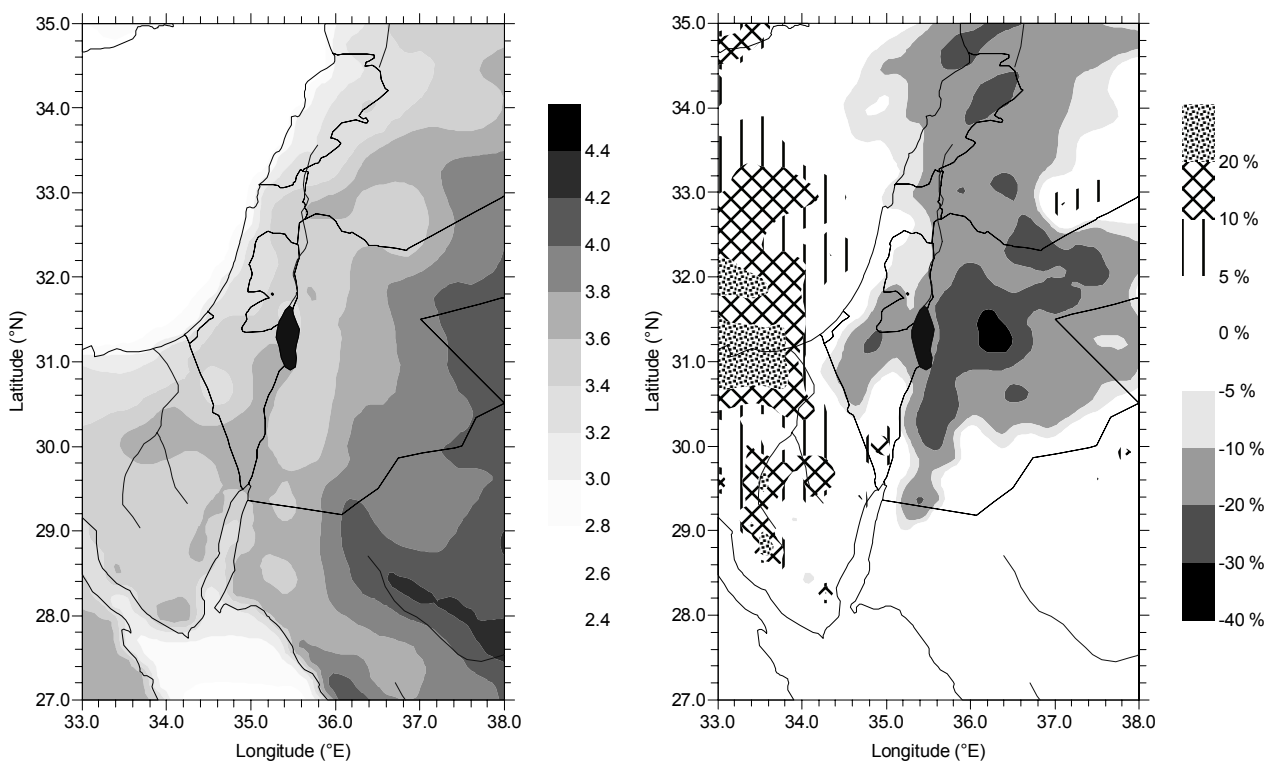


Fig. 3 Predicted changes in mean annual temperature ($^{\circ}\text{C}$, left) and precipitation (%), right) (2070–2099 vs 1961–1990).

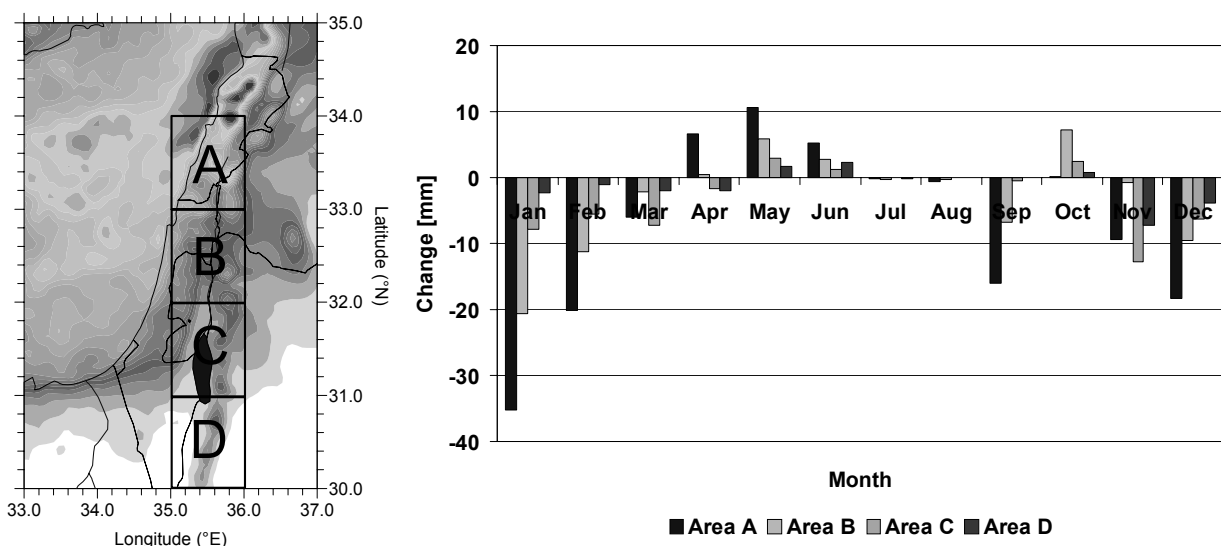


Fig. 4 Predicted change in precipitation for the four subregions (2070–2099 vs 1961–90).

vegetation specifically calculated according to Penman-Monteith (Monteith, 1975; Brutsaert, 1982). Interception is accounted for by a bucket approach. Snow accumulation and snowmelt is determined according to Anderson (1973) and Braun (1985). Surface runoff is created for each grid cell as the sum of infiltration excess and snowmelt and routed along the topographic gradient towards the river. It is assumed that saturated hydraulic conductivity decreases (dependent on soil texture) with depth

according to a recession constant. Discharge routing is performed by a kinematic wave approach using different flow velocities for different water levels in the channel. After the translation of the wave, a single linear storage is applied to the routed discharge considering diffusion and retention (Schulla & Jasper, 2000). WaSiM was applied with an integrated 2D groundwater flow model, which couples dynamically to the unsaturated zone. The uppermost (and in this study single) aquifer is assumed to be unconfined. Infiltration from rivers into groundwater and exfiltration (which is the baseflow) from groundwater into rivers is calculated using the hydraulic gradient and representation of colmation processes (in- and exfiltration resistance) at the river bed.

The river courses were derived from a digital elevation model with 90 m resolution (based on SRTM satellite mission digital elevation data). River discharge information for six gauges (Ayun, Snir, Dan, Banyas, Saar, and the Jordan at Yoseph's bridge) are available for this study. The unsaturated zone was discretized to a maximum depth of 100 m. Gridded soil data were compiled from Israeli national data sets (resolution 1:500 000; provided by the Kinneret Limnological Laboratory) and from FAO data (resolution 1:1 500 000) for the Syrian and Lebanese part of the UJC. Gridded land-use information was also obtained from Israeli national data sets (25 m resolution) and derived from MODIS satellite information (1 km resolution) for Syrian and Lebanon parts of the UJC. Six different soil textures and eight different land-use types were distinguished within the catchment. Outflow of groundwater across the eastern (surface water) boundary located along Mount Hermon and at the northeastern edge of the Snir subcatchment, were quantified following Gur *et al.* (2003). The Dan, El-Wazani, Hazbani and Banyas springs are represented by constant groundwater heads.

Because the hydrological model is not able to account for the karstic environment and corresponding preferential flow paths, which are typical of the Mount Hermon region (e.g. Rimmer & Salingar, 2006), water flow is instead approximated assuming porous conditions. The model set-up therefore represents a substitutional porous media whose parameters must be interpreted as effective lumped parameters approximating the karstic environment on a subcatchment scale.

Hydrological modelling of the UJC is also hampered by the limited availability of daily meteorological station data. While in the Israeli part of the catchment, only two precipitation stations and no climatological stations were available, no daily station data were accessible in the Syrian and Lebanese part of the catchment. Instead data from six Israeli precipitation stations and two climatological stations located outside of the catchment were applied. In Syria, Lebanon and Jordan, data from nine precipitation stations and six climatological stations located outside the catchment (up to a maximum distance of 80 km from the catchment) were used. Gridded daily meteorological fields were obtained by a combination of inverse distance weighting and height-dependent regression of station values. Because the amount of precipitation on the elevated regions of Mount Hermon (>1200 m a.s.l.) was never measured systematically, estimations of snow and rainfall in this study were based on stations located at much lower elevations.

The subcatchments and a comparison between modelled and observed discharge for the Yoseph Bridge gauge are shown in Fig. 5. Overestimation of simulated discharge of the Jordan at Yoseph Bridge during summer months is due to the fact that upstream water consumption and technically bypassed freshwater was not accounted

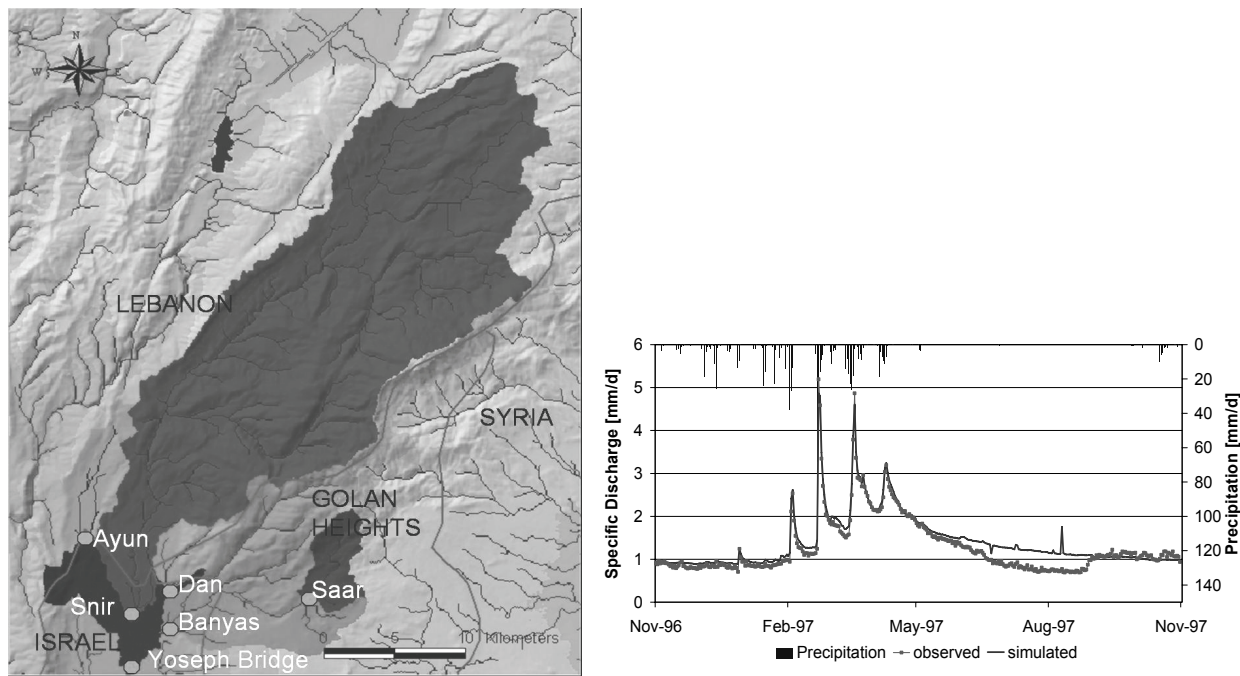


Fig. 5 Location of subcatchments and respective gauges of Upper Jordan catchment (left) and comparison between simulated and observed discharge at the Yoseph Bridge gauge for the 1997 hydrological year.

for in the current hydrological model data. Considering these constraints it is concluded that the hydrological model is able to simulate the streamflow in the UJC satisfactorily. Current and envisaged future research focuses on additional validation of model performance using groundwater observations and environmental tracer information.

RESULTS OF JOINT CLIMATE–HYDROLOGY SIMULATIONS

Meteorological fields of precipitation, wind speed, relative humidity, temperature and shortwave radiation are passed from the MM5 results to the hydrological model. In the case of temperature and precipitation, a combination of height-dependent regression and inverse distance weighting is applied to interpolate meteorological fields from the meteorological model resolution to the resolution of the hydrological model.

Figure 6 shows the simulated annual mean temperature for the two time slices (left) and the predicted change in temperature (right). Temperature increase is of the order of 4.5°C in the eastern part of the catchment (i.e. the mountainous region of Mount Hermon), and around 3°C in the southwestern part of the catchment, i.e. the Hula valley. Figure 7 shows likewise the simulated mean annual precipitation and the predicted changes. The precipitation decrease is around 10% in the lower regions and reaches around 25% in the mountainous regions.

Figure 8 (left) shows that the simulated change in total runoff at the outlet of the catchment (Yoseph Bridge) is expected to decrease by as much as 40% in winter months. Figure 8 (right) shows the predicted change in groundwater recharge. Changes in groundwater recharge are slightly amplified compared to changes in total runoff.

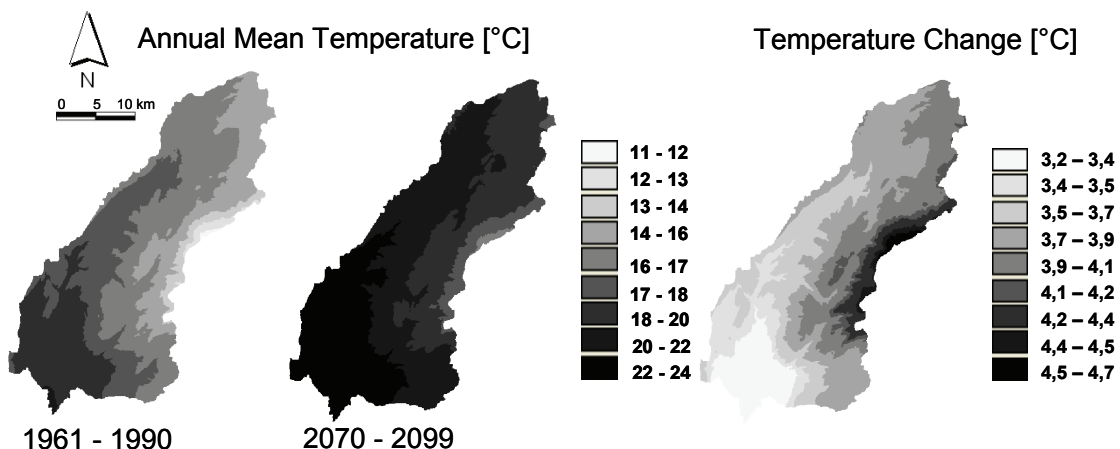


Fig. 6 Simulated mean annual temperature for the two time slices and relative change, in %, for the UJC.

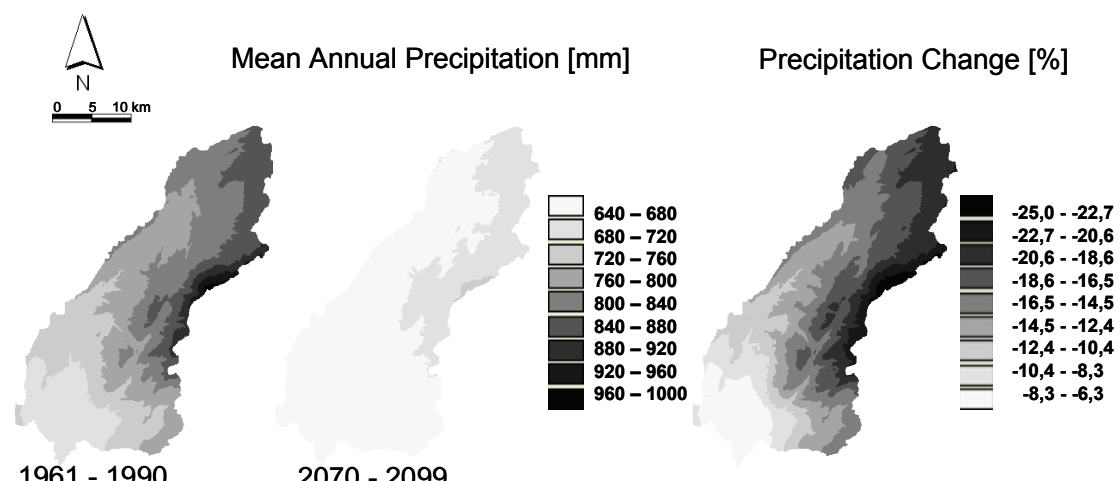


Fig. 7 Simulated mean annual precipitation for the two time slices and relative change, in %, for the UJC.

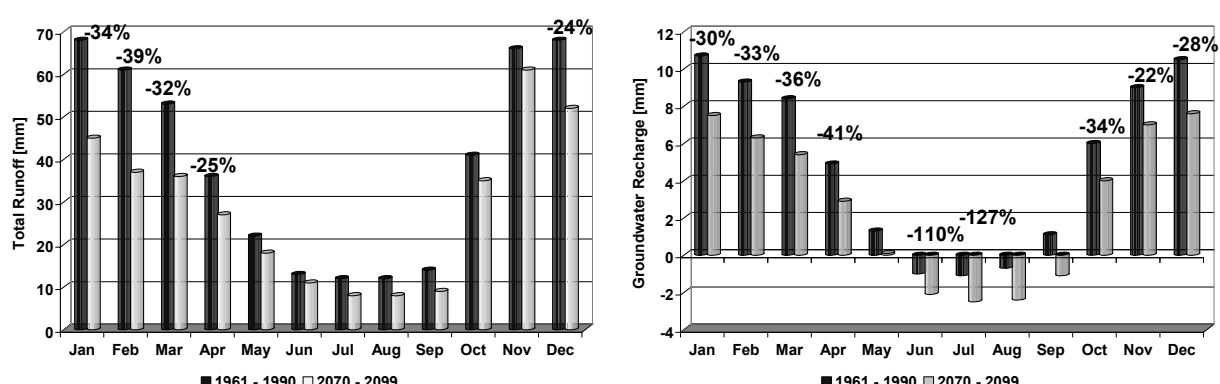


Fig. 8 Temporal distribution of total runoff (left) and groundwater recharge (right) in the UJC (2070–2099 vs 1961–1990).

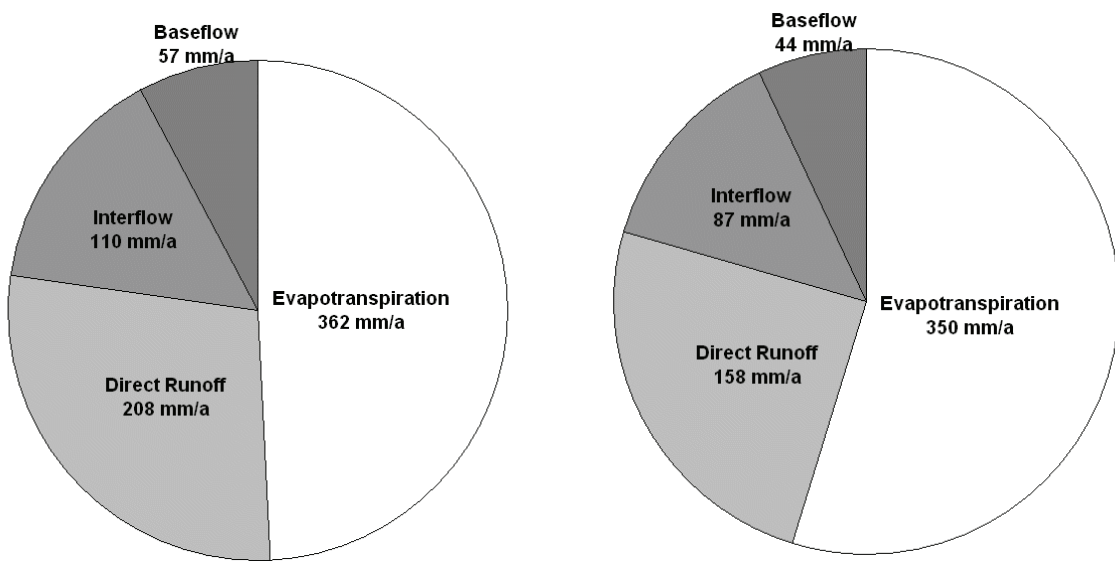


Fig. 9 Changes in water balance variables: 1961–1990 (with a mean annual precipitation of 788 mm/year; left) vs 2070–2099 (670 mm/year, right). Residuals in water balance (51 mm, left, respectively 31 mm, right) are due to modelled outflow of groundwater across the surface water boundary.

Again, significant reductions are expected. Figure 9 shows the change in the overall water balance. The mean annual sum of total runoff and evapotranspiration is decreased from 737 mm (1961–1990) to 639 mm (2070–2099), i.e. by around 100 mm (corresponding to 13%). Due to higher air temperatures, the relative fraction of evapotranspiration to total water availability increases from 49% to 54%. Total runoff is decreased by 23% (from 375 mm/year to 289 mm/year).

SUMMARY AND CONCLUSIONS

Regional climate simulations based on the global climate scenario B2 of ECHAM4 were dynamically downscaled to a final resolution of 18 km. Results were applied to drive a distributed hydrological model allowing us to simulate the expected changes in the terrestrial water balance for the UJC. Results of the joint regional climate–hydrology simulations indicate an increasing mean annual temperature of up to 4.5°C and a decrease of mean annual precipitation by as much as 25%, in the UJC. Total runoff is expected to decrease by 23%, and is accompanied by significant decreasing groundwater recharge. The results show a significant decrease of water availability in the region which will have tremendous consequences for water management. Future work will focus on applying the joint climate–hydrology modelling system to further emission scenarios and different global models (e.g. HadCM3) to investigate uncertainty bounds for the derived trends and expected changes.

REFERENCES

- Anderson, E. (1973) National Weather River Forecast System – Snow Accumulation and Ablation Model. *NOAA Tech. Mem. NWS-Hydro-17*. US Department of Commerce, USA.

- Braun, L. N. (1985) Simulation of snowmelt-runoff in lowland and lower alpine regions of Switzerland. *Zürcher Geographische Schriften*, 21. ETH Zürich, Switzerland.
- Brutsaert, W. (1982) *Evaporation into the Atmosphere*. Kluwer Academic Publishers, Dordrecht, The Netherlands.
- Chen, F. & Dudhia, J. (2001) Coupling an advanced land-surface/hydrology model with the Penn State/NCAR MM5 modeling system. Part I: Model implementation and sensitivity. *Mon. Weath. Rev.* **129**, 569–585.
- Grell, G., Dudhia, J. & Stauffer, D. (1994) A description of the fifth-generation Penn State/NCAR Mesoscale Model (MM5). *NCAR Technical Note*, NCAR/TN-398+STR.
- Green, W. H. & Ampt, G. A. (1911) Studies on soil physics: I. The flow of air and water through soils. *J. Agric. Sci.* **4**, 1–24.
- Gur, D., Bar-Matthews, M. & Sass, E. (2003) Hydrochemistry of the main Jordan River sources: Dan, Banias, Kezinim springs, north Hula Valley, Israel. *Israel J. Earth Sci.* **52**, 155–178.
- Hon, S. & Pan, H., (1996) Nonlocal boundary layer vertical diffusion in a medium-range forecast model. *Mon. Weath. Rev.* **124**(10), 2322–2339.
- Kunstmann, H., Schneider, K., Forkel, R. & Knoche, R. (2004) Impact analysis of climate change for an alpine catchment using high resolution dynamic downscaling of ECHAM4 time slices. *Hydrol. Earth System Sci.* **8**(6), 1030–1044.
- Monteith, J. L. (1975) *Vegetation and the Atmosphere*, vol. 1: *Principles*. Academic Press, London, UK.
- Peschke, G. (1987) Soil moisture and runoff components from a physically founded approach. *Acta Hydrophysica* **31**(3/4), 191–205.
- Phillip, J. R. (1969) The theory of infiltration. In: *Advances in Hydrosciences* (ed. by V. T. Chow), 216–296. Academic Press, New York, USA.
- Reisner, J., Rasmussen, J. & Bruntjes, R. (1998) Explicit forecasting of supercooled liquid water in winter storms using the MM5 mesoscale model. *Quart. J. Roy. Met. Soc.* **124B**, 1071–1107.
- Richards, L. A. (1931) Capillary conduction of liquids through porous medium. *Physics* **1**, 318–333.
- Rimmer, A. & Salingar, Y. (2006) Modelling precipitation-streamflow processes in karst basin: the case of the Jordan River sources, Israel. *J. Hydrol.* **331**, 524–542.
- Schulla J. & Jasper, K. (2000) *Model Description WASIM-ETH* (Water Balance Simulation Model ETH). ETH Zurich, Zurich, Switzerland.
- Van Genuchten, M. T. (1976) A closed form equation for predicting the hydraulic conductivity of unsaturated soils. *Am. J. Soil Sci.* **44**(5), 892–898.